A High-Frequency Flying-capacitor Linear Amplifier for Wireless Power Transfer Systems

Shunsaku Nomoto, Rintaro Kusui, Keisuke Kusaka
Dept. of Electrical, Electronics, and Information Engineering
Nagaoka University of Technology
Nagaoka, Japan
s201067@stn.nagaokaut.ac.jp, kusui@stn.nagaokaut.ac.jp, kusaka@vos.nagaokaut.ac.jp

***Abstract*— Wireless power transfer (WPT) systems emit leakage magnetic fields due to their operating principle. Thus, reducing electromagnetic field (EMF) harmonics is essential to meet standards such as CISPR. The WPT system with a flying capacitor linear amplifier (FCLA) has been proposed to reduce the EMF. However, the high-frequency operation of the FCLA has not yet been realized. This paper proposes a gate driver unit (GDU) that enables the high-frequency operation of the FCLA with low voltage distortion by feedforward compensation of the gate-source voltage. Experimental results show that the WPT system with a 2-series FCLA prototype reduces odd harmonic components of primary current by up to 16.5 dB compared to the conventional WPT system with a square-wave output inverter.**

Keywords*— linear amplifier, flying capacitor converter, wireless power transfer, Electromagnetic field (EMF)

I. INTRODUCTION

Electric vehicles (EVs) have gained significant popularity in global efforts to reduce fossil fuel consumption and minimize environmental impacts. EVs can have a much smaller carbon footprint depending on how electricity is generated than conventional internal combustion engine (ICE) vehicles. Additionally, these vehicles offer potential cost savings through lower operating expenses.

As an alternative to traditional wired charging systems, wireless power transfer (WPT) has been introduced for charging EV batteries [1–3]. WPT offers the advantage of contactless charging, simplifying the process, and improving the convenience of EVs. Moreover, WPT improves safety when charging EV batteries in environments with water or other conductive materials. However, WPT systems emit a leakage magnetic field due to the weak magnetic coupling between the transmitting and receiving coils [4–6]. This electromagnetic field (EMF) can damage human health and interfere with the proper operation of electric devices. The International Special Committee on Radio Interference (CISPR) has published reference levels of radiation noise in order to prevent the malfunction of wireless communication and electric devices [7]. Most WPT systems use a full-bridge inverter with square-wave output as the power supply. As a result, these systems emit radiation noise due to low-order harmonic currents. Thus, reducing the harmonic currents through the coils is necessary to satisfy the above standard.

References [8, 9] have proposed adding coils to reduce the harmonic components of EMF due to the harmonic currents that flow WPT coils. However, these methods need additional windings near the WPT coils. As a result, these coils reduce not only the harmonic leakage field but also the magnetic field's fundamental component. This is a factor that reduces the coupling of the WPT coils. Thus, it is challenging to achieve both efficiency and the effect of reducing the EMF harmonic.

Ref. [10] has also proposed a reduction method for harmonic EMFs. This method reduces harmonic currents that cause harmonic EMFs by applying a flying-capacitor linear amplifier (FCLA) as a power supply for WPT systems. FCLA outputs continuous voltage with high efficiency [10, 11]. Thus, WPT systems with FCLA output sinusoidal voltage that contains no harmonics. As a result, no harmonic current flows WPT coils and almost no harmonic EMF is emitted from the WPT system. However, the WPT with the FCLA has not yet been demonstrated because an operating method of the FCLA at high frequencies has not been revealed. A gate driver unit (GDU) in [10] has a feedback loop to control the output of the FCLA. This feedback loop includes a time delay, which leads to the destabilization of the control system. Hence, it is difficult to increase the bandwidth of the GDU and output a high-frequency command. Additionally, another proposed method operates the FCLA in an open loop by connecting the GDU between the drain and gate [11]. While this method is not limited by the control system bandwidth of the GDU for the operating frequency, it has not yet established a way to compensate for the nonlinear characteristics of the MOSFET. Thus, this method may not achieve high-frequency output with low distortion.

This paper proposes a GDU that outputs a voltage for the FCLA operation at high frequencies. The proposed GDU operates in an open loop with a feedforward control of the gate-source voltage. The gate-source voltage is a source of output voltage distortion and varies nonlinearly with the operating state of the MOSFET. Thus, this feedforward is necessary to achieve high-frequency output with low distortion in FCLA. The prototype of a WPT system with FCLA demonstrates that the prototype reduces harmonic current that flows in a primary coil of the WPT system compared to a traditional WPT system that has a square output inverter. The new contribution of this paper is enabling the FCLA to achieve a high-frequency sinusoidal voltage output with low distortion by feedforward control.

II. FCLA FOR WPT SYSTEM

A. System Configuration

Figure 1 shows the system configuration of a WPT system with the FCLA. The system consists of n-series FCLA, n n-MOSFETs, n diodes, an unfolder, resonant capacitors, and WPT coils [10]. A traditional switching power converter uses MOSFETs in only ON (saturation region) and OFF (cutoff region) operations. On the other hand, FCLA uses three operation modes: ON, OFF, and active (active region) mode. Due to this, FCLA output continuous voltage. The unfolder outputs a sinusoidal voltage by switching the polarity of the full-wave rectified voltage of the FCLA output. The active mode of MOSFETs results in large losses compared to the ON mode because of a high drain-source voltage. However, increasing the number of MOSFETs improves the power conversion efficiency of FCLA because the drain-source voltage decreases on MOSFET in active mode. Thus, the FCLA outputs a sinusoidal voltage without harmonics with high efficiency.

The FCLA has multiple operation modes that output a certain voltage. Figure 2 shows the current paths in the case of 2-series FCLA. The Flying capacitor (FC) is balanced at half the DC supply voltage ($V_{DC}/2$) in Fig. 2. The number of MOSFET in the OFF mode determines the output voltage, as shown in (1).

$$\frac{n-k-1}{n}V_{DC} < v_{out} < \frac{n-k}{n}V_{DC} \qquad (1),$$

where k is the number of series MOSFETs in OFF mode, a continuous voltage output is achieved when any MOSFETs enters active mode. The current path changes depending on the operation mode of MOSFETs. Thus, an isolated GDU on each series MOSFET allows FCLA to maintain balanced FC voltages.

B. Control Scheme

Selecting appropriate operation modes of MOSFETs enables the FCLA to maintain balanced FC voltages, as shown in Fig. 2. Current paths for charging or discharging FCs are controlled by selecting the operation mode of MOSFETs according to the output voltage and current. However, the degrees of freedom for selecting current paths increases as the number of series-connected MOSFETs n grows. This degree of freedom makes it challenging to choose the appropriate combination of operation modes of MOSFETs that maintain the FC voltage balance.

To address this issue, phase-shifted carriers select the operating modes of the MOSFETs [10]. Figure 3 shows the control scheme of each series MOSFET for a 4-series FCLA. Equation (1) determines the output voltage of a FCLA. Three operation modes are selected by comparing phase-shifted carriers with two thresholds that depend on the output command of the FCLA. The threshold for the OFF mode varies in 1/n steps depending on the FCLA output voltage command. The ON mode threshold is 1/n smaller than the OFF mode one. If the carrier is less than the ON mode threshold, the MOSFET becomes the ON mode. If the carrier exceeds the OFF-mode threshold, the MOSFET becomes the OFF mode. If neither of the above two cases applies, the MOSFET is in the active mode. Carriers with a frequency asynchronous to output frequency allow the FCLA to select different current paths within a few cycles. Consequently, the FCLA keeps balanced FC voltages.

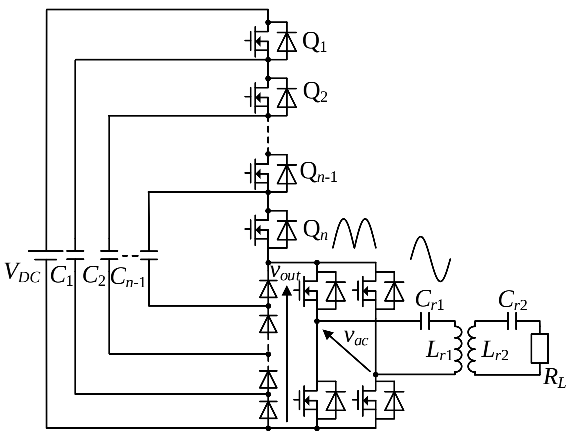

Fig. 1. The circuit configuration of a WPT system with a flying capacitor linear amplifier.

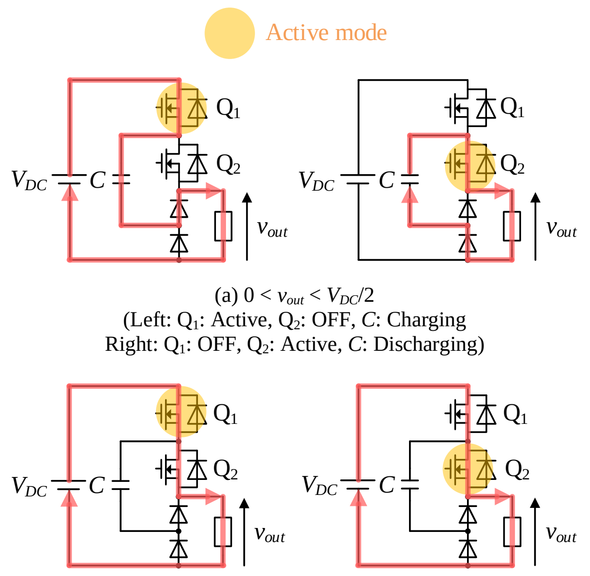

(a) $0 < v_{out} < V_{DC}/2$
(Left: Q_1: Active, Q_2: OFF, C: Charging
Right: Q_1: OFF, Q_2: Active, C: Discharging)

(b) $V_{DC}/2 < v_{out} < V_{DC}$
(Left: Q_1: Active, Q_2: ON, C: No charging or discharging
Right: Q_1: ON, Q_2: Active, C: No charging or discharging)

Fig. 2. Current paths of a 2-series flying-capacitor linear amplifier.

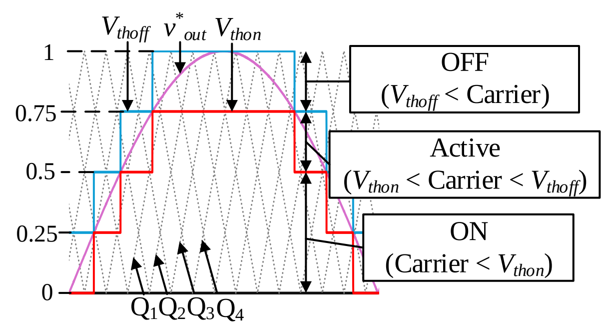

Fig. 3. Mode selection for balanced flying-capacitor voltages.

III. PROPOSED GDU FOR HIGH-FREQUENCY FCLA

This chapter explains the proposed GDU for high-frequency operation. The proposed GDU is improved to achieve the high-frequency operation based on the GDU proposed in [11].

Ref. [11] proposes a method to control the FCLA by connecting the GDU between the drain and gate of the MOSFET. Figure 4 shows the operation principle of a source follower. Each MOSFET in the FCLA operates as a source follower to output continuous voltage. As a result, the source voltage follows the gate voltage of each MOSFET. Thus, the drain-source voltage of the MOSFETs is directly controlled by GDUs connected to the drain-gate. However, the source voltage does not fully follow the gate voltage. There is always a discrepancy equal to the gate-source voltage between the gate and source terminals. Furthermore, the gate-source voltage varies nonlinearly because of the threshold voltage, the channel length modulation effect, and the stray capacitance of MOSFETs. Ref. [11] does not consider how to compensate for the nonlinear characteristics of MOSFETs. Thus, this method may not achieve high-frequency output with low distortion.

Therefore, the proposed GDUs for the FCLA have feedforward control for the gate-source voltage to compensate for the discrepancy. Figure 5 shows the proposed GDU for a high-frequency output. This GDU has the reference electric potential as the potential at the gate terminal of the MOSFET and employs feedforward control that manipulates the drain-gate voltage by detecting the gate-source voltage. The drain-source voltage of each MOSFET is expressed as

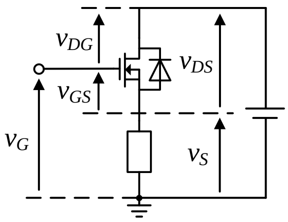

(a) Circuit diagram.

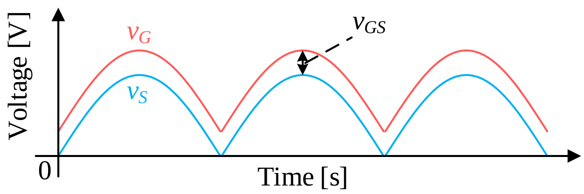

(b) Operation waveforms.

Fig. 4. The operation principle of a source follower.

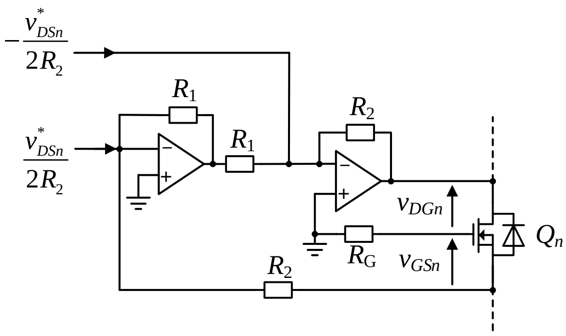

Fig. 5. The configuration of the proposed gate driver unit.

$$v_{DS} = v_{DG} + v_{GS} \qquad (2),$$

where v_{DS} is the drain-source voltage, v_{DG} is the drain-gate voltage, and v_{GS} is the gate-source voltage. The drain-source voltage command should subtract the detected gate-source voltage value to control the drain-source voltage by the drain-gate voltage of the MOSFET from (2). The output of the GDU is expressed as

$$v_{DGn} = -\left\{-\frac{v^*_{DSn}}{2R_2} - \left(\frac{v^*_{DSn}}{2R_2} - \frac{v_{GSn}}{R_2}\right)\right\} R_2 \qquad (3),$$

$$v_{DGn} = v^*_{DSn} - v_{GSn} \qquad (4),$$

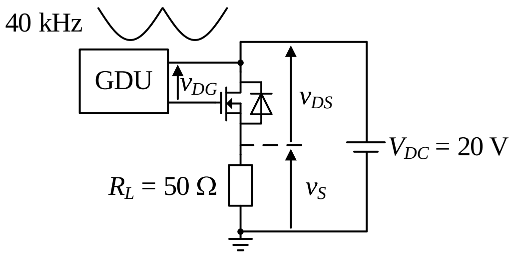

Fig. 6. The simulation condition of a source follower.

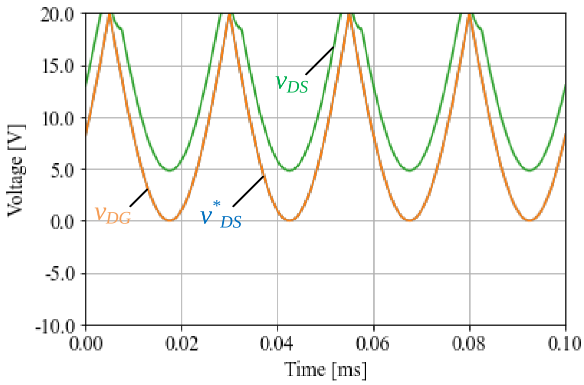

(a) Waveforms of MOSFET (v^*_{DS}: Drain-source voltage command).

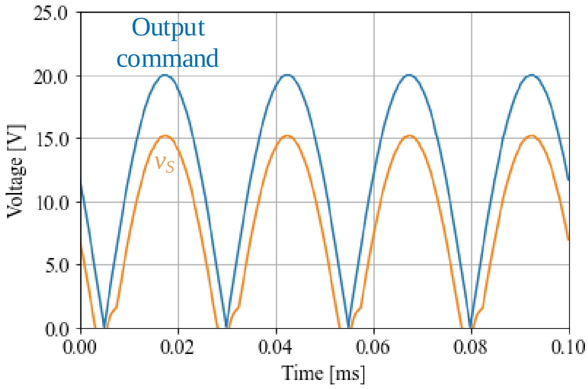

(b) Output of the source follower.

Fig. 7. Operation waveforms of the source follower with the conventional gate driver unit.

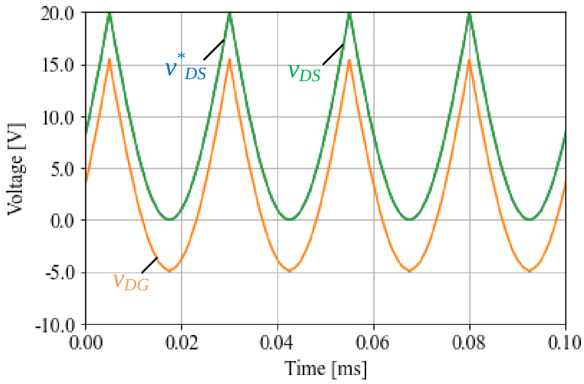

(a) Waveforms of MOSFET (v^*_{DS}: Drain-source voltage command).

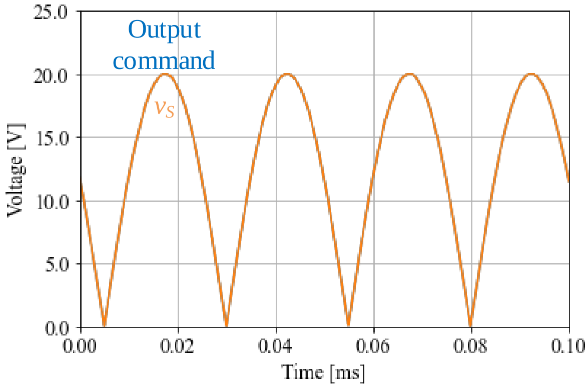

(b) Output of the source follower.

Fig. 8. Operation waveforms of the source follower with the proposed gate driver unit.

where v_{DGn}, v_{GSn}, and v^*_{DSn} are Q_n's drain-gate voltage, gate-source voltage, and drain-source command. The proposed GDU compensates for the nonlinear characteristics of MOSFETs.

IV. Simulation of the Proposed Method

A. Proposed GDU

A simulation is conducted using a source follower to validate the proposed GDU's effect. Figure 6 shows the simulation condition. Figures 7 and 8 show simulation results of the operating waveforms when the conventional and proposed GDU gives the MOSFET a 40 kHz full-wave rectified voltage command. Since the conventional GDU has an output equal to the drain-source voltage command, there is an error between the drain-source voltage and the command as shown in (2). It results in the source follower with conventional GDU outputs a voltage different from the output command. In comparison, the source follower with the proposed GDU outputs a voltage necessary to control the drain-source voltage as commanded. The voltage between the GDU output and the drain-source voltage command value varies with the command value because MOSFETs have nonlinear characteristics. The proposed GDU enables a MOSFET to output voltage following the command with low distortion by feedforward of the gate-source voltage.

B. WPT systems with FCLA

Figures 9 and 10 show the operation waveforms of the proposed WPT system with an FCLA as shown in Fig. 1. Table 1 shows simulation conditions. The FCLA outputs sinusoidal voltage and current while switching the operation mode of MOSFETs based on Fig. 3 generates a surge voltage on the primary side of the WPT system. The proposed FCLA operates in the WPT system. In addition, each FC maintains balanced voltages.

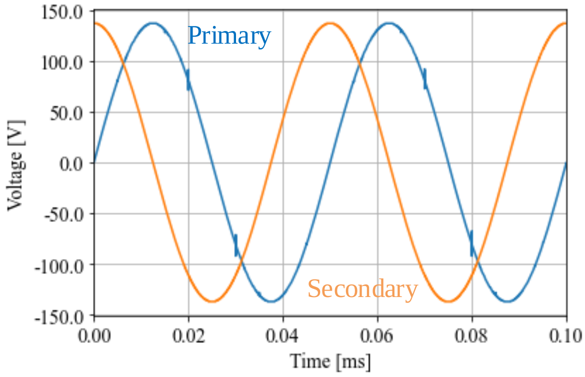

(a) WPT primary and secondary voltage.

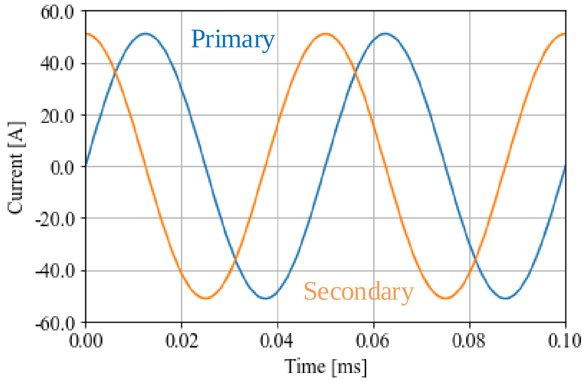

(b) WPT primary and secondary current.

Fig. 9. The operation waveforms of the WPT system with the 4-series flying-capacitor linear amplifier.

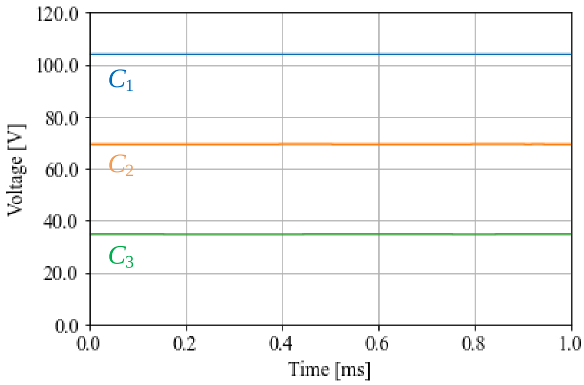

Fig. 10. Flying-capacitor voltage balance of the WPT system.

Figure 11 shows the comparison of the harmonic currents of the traditional and FCLA-equipped WPT systems. The WPT system with 4-series FCLA reduces odd harmonic components of output current by up to 69.5 dB compared to the traditional WPT system with a square output inverter.

Table 1. Simulation conditions of the WPT system with the 4-series flying-capacitor linear amplifier.

Parameter	Symbol	Value
Power	P	3.7 kW
DC voltage	V_{DC}	141 V
Frequency	f	20 kHz
Capacitance of a flying capacitors	C_1, C_2, C_3	10 μF
Capacitance of resonant capacitors	C_{r1}, C_{r2}	592.4 nF
Inductance of coils	L_{r1}, L_{r2}	106.9 μH
Coupling	k	0.20
Load resistor	R_L	2.69 Ω
Number of series	n	4

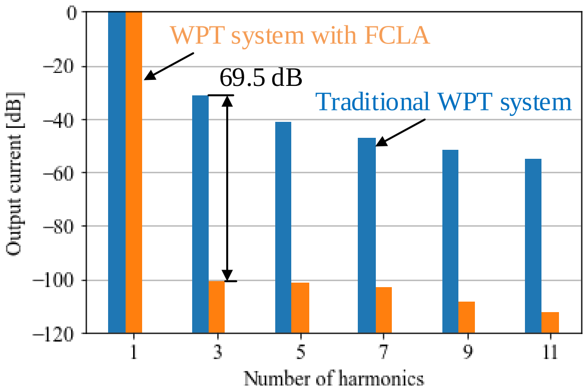

Fig. 11. Harmonic analysis for the primary current.

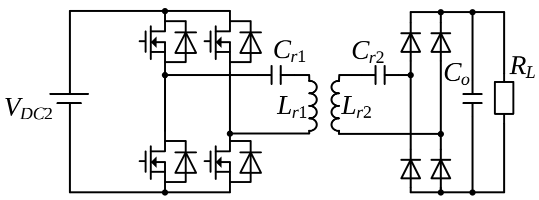

(a) Conventional.

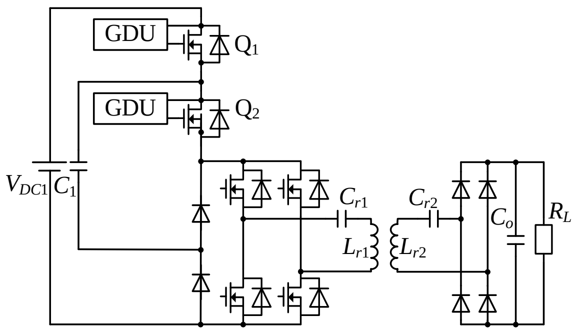

(b) With the 2-series flying-capacitor linear amplifier.

Fig. 12. Prototypes of conventional and FCLA-equipped WPT systems.

Table 2. Circuit parameters of the conventional and FCLA-equipped WPT system.

Parameter	Symbol	Value
DC voltage	V_{DC1}	20 V
DC voltage	V_{DC2}	16 V
Frequency	f	20 kHz
Capacitance of a flying capacitor	C_1	10 μF
Capacitance of resonant capacitors	C_{r1}, C_{r2}	156.1 nF
Inductance of primary coil	L_{r1}	415.6 μH
Inductance of secondary coil	L_{r2}	414.0 μH
Coupling	k	0.134
Load resistor	R_L	8.5 Ω

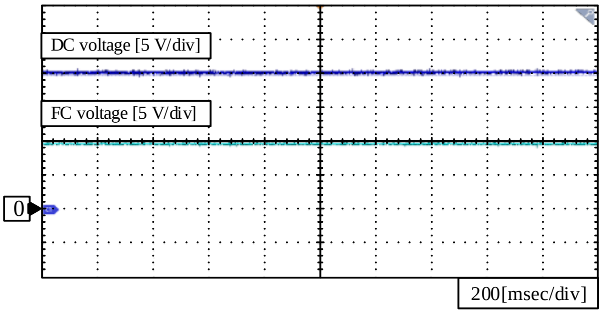

Fig. 13. Flying-capacitor (FC) voltage balance.

V. Experimental Results

A. Prototype system

A comparison was conducted between the conventional WPT system and the FCLA-equipped system that has the proposed GDU to verify the effectiveness of the WPT system with FCLA in suppressing current harmonics in the transmission coils. Figure 12 shows circuit diagrams of the conventional and WPT systems with FCLA. The conventional WPT system consists of a full-bridge inverter with a square output, resonant capacitors, transmitting and receiving coils, a rectifier, and load resistance. The WPT system uses the FCLA as the primary power source for the WPT system. Table 2 shows the circuit parameters of prototypes of WPT systems. DC supply voltages of the conventional and FCLA-equipped WPT systems are different to equalize the transmission power.

B. Validation of the Proposed Method

Figure 13 shows the operation waveforms of the 2-series FCLA prototype. The FC voltage is balanced by applying the balance control as shown in Fig. 3.

Figure 14 shows the operation waveforms of the conventional and FCLA-equipped WPT system. The prototypes of WPT systems are resonated at the inverter output frequency by the resonant capacitors. Furthermore, even if the FCLA is applied to a WPT system, it operates normally and outputs a sinusoidal voltage with low distortion.

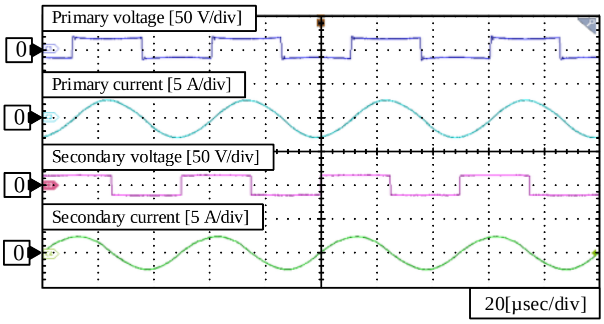

(a) Conventional.

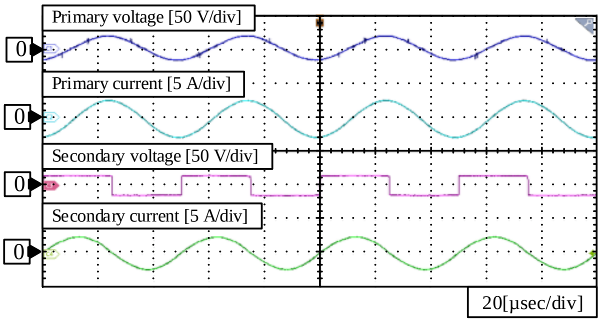

(b) With 2-series flying-capacitor linear amplifier.

Fig. 14. Operation waveforms of the prototypes of WPT systems.

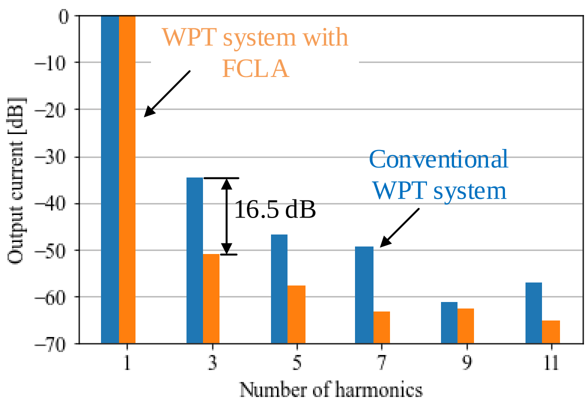

Fig. 15. Harmonic analysis for the primary current of the prototypes.

Figure 15 shows the comparison of the harmonic currents of the traditional and FCLA-equipped WPT system prototype. The WPT system prototype with 2-series FCLA reduces odd harmonic components of output current by up to 16.5 dB compared to the conventional WPT system prototype. The prototypes have a rectifier, and the secondary voltage becomes a square wave regardless of the primary side. Thus, the effect of reducing current harmonics is smaller than in the system configuration shown in Fig. 1.

VI. Conclusion

A WPT system with FCLA has been proposed to reduce the harmonic components of primary current for WPT systems. However, the high-frequency operation of the FCLA has not yet been realized so far. The proposed GDU enables the FCLA to achieve a high-frequency output because of feedforward control without feedback. The prototype of the WPT system with 2-series FCLA transfers power with 20 kHz sinusoidal voltage with low distortion and reduces odd harmonic components of output current by up to 16.5 dB compared to the conventional WPT system with a square output inverter.

Acknowledgment

This work is partially supported by the New Energy and Industrial Technology Development Organization (NEDO) under the project titled "Support Program for Young Researchers through Public-Private Partnership / Matching Support Phase (Environment and Energy Field) / Leakage Magnetic Field Reduction in High-Power Wireless Power Transfer by Multilevel Linear Amplifier" (Project No.: 24000773-0).

References

[1] Keisuke Yamamoto, Jun Enomoto, Shunsaku Koga, Junichi Kitano, "Theoretical Consideration of the Long-length Primary Loop used in SCMaglev's DWPT System," in IEEJ Journal of Industry Applications, vol. 13, no. 5, pp. 580-586, July, 2024.

[2] R. Qin, J. Li, J. Sun and D. Costinett, "Shielding Design for High-Frequency Wireless Power Transfer System for EV Charging With Self-Resonant Coils," in IEEE Transactions on Power Electronics, vol. 38, no. 6, pp. 7900-7909, June 2023.

[3] H. Zhao et al., "Shielding Optimization of IPT System Based on Genetic Algorithm for Efficiency Promotion in EV Wireless Charging Applications," in IEEE Transactions on Industry Applications, vol. 58, no. 1, pp. 1190-1200, Jan.-Feb. 2022.

[4] M. Mohammad, E. T. Wodajo, S. Choi and M. E. Elbuluk, "Modeling and Design of Passive Shield to Limit EMF Emission and to Minimize Shield Loss in Unipolar Wireless Charging System for EV," in IEEE Transactions on Power Electronics, vol. 34, no. 12, pp. 12235-12245, Dec. 2019.

[5] Keisuke Kusaka, Kazuki Yamagata, Jin Katsuya, Tetsu Sato, "Reduction in Leakage Magnetic Flux of Wireless Power Transfer Systems with Halbach Coils," in IEEJ Journal of Industry Applications, vol. 12, no. 6, pp. 1104-1105, Nov. 2023.

[6] X. Zan and A. -T. Avestruz, "Field Cancellation for Circuits Encircled by VHF Wireless Power Transfer Coils," in IEEE Transactions on Power Electronics, vol. 38, no. 1, pp. 46-52, Jan. 2023.

[7] International special committee on radio interference (CISPR 11), Industrial, scientific and medical equipment – Radio-frequency disturbance characteristics – Limits and methods of measurement, 2019.

[8] S. Hong et al., "A Frequency-Selective EMI Reduction Method for Tightly Coupled Wireless Power Transfer Systems Using Resonant Frequency Control of a Shielding Coil in Smartphone Application," in IEEE Transactions on Electromagnetic Compatibility, vol. 61, no. 6, pp. 2031-2039, Dec. 2019.

[9] C. Lee, S. Woo, Y. Shin, J. Rhee, J. Moon, and S. Ahn, "EMI Reduction Method for Wireless Power Transfer Systems With High Power Transfer Efficiency Using Frequency Split Phenomena," in IEEE Transactions on Electromagnetic Compatibility, vol. 64, no. 5, pp. 1683-1693, Oct. 2022.

[10] R. Kusui, K. Kusaka and J. -I. Itoh, "Flying-capacitor Linear Amplifier for Wireless Power Transfer Systems with Flying-capacitor Voltage Balancing," 2021 23rd European Conference on Power Electronics and Applications (EPE'21 ECCE Europe), Ghent, Belgium, 2021, pp. P.1-P.9.

[11] H. Obara and K. Matsushima, "A Study on Flying Capacitor Linear Amplifier Configured by Only N-channel MOSFETs," 2021 IEEE International Future Energy Electronics Conference (IFEEC), Taipei, Taiwan, 2021, pp. 1-5.